Preprints of the 19th World Congress
The International Federation of Automatic Control
Cape Town, South Africa. August 24-29, 2014

Estimation of the Possible Power of a Wind Farm

Mahmood Mirzaei * **Tuhfe Göçmen** ** **Gregor Giebel** **
Poul Ejnar Sørensen ** **Niels K. Poulsen** *

* *Department of Applied Mathematics and Computer Science, Technical University of Denmark, Denmark,* {mmir, npko}@dtu.dk
** *Department of Wind Energy, Risø, Technical University of Denmark, Denmark,* {tuhf, grgi, posq}@dtu.dk

Abstract: It seems possible to increase competitiveness of wind power plants by offering grid services (also called ancillary services) and enter the wind power plants into the ancillary market. One of the ancillary services is called reserve power, the differential capacity between the generated power and the available power in the farm. The total amount of energy that a wind farm can potentially generate is called possible power. It is very important for a wind farm owner to have a relatively accurate estimate of the possible power of the wind farm in order to be able to trade the reserve power. In this paper the possible power calculated based on the estimated effective wind speed of a down regulated wind farm (the industry standard) is compared against the calculated possible power based on the algorithm presented in the paper. The latter takes into account the effect of the wakes of down regulated turbines and therefore gives a more accurate measure of the possible power. It is shown that for an interval of wind speeds the difference between these two can increase the uncertainty in the estimate of the possible power of the down regulated wind farm.

Keywords: Power systems, wind farm, possible power, wind speed estimation, wake models

1. INTRODUCTION

It seems possible to increase competitiveness of wind power plants by offering grid services (also called ancillary services) and enter the wind power plants into the ancillary market, see (Miller and Clark, 2010). This will result in better incentives for power plant owners to employ wind turbines even more. Besides, in some countries such as Denmark and Ireland as the penetration of the wind energy in the utility grid is increasing, participation of wind turbines and wind farms in the ancillary services for power grid stability has become inevitable, see (Hansen, 2010). The ancillary services are normally provided by traditional power plants, however with proper controller design wind power plants can also contribute to the ancillary services, (Miller and Clark, 2010). The special nature of wind turbines enables them to provide some of the services for grid stability even better than the traditional power plants. For example due to the nature of the wind turbines, their power can be ramped up quickly. Besides because of the big inertia in the rotor and the generator of the turbine, if designed properly, they can provide inertial response to the grid, (Aho et al., 2012). For a survey on frequency and voltage control and information on inertial responses, see (Rebours et al., 2007). One of the ancillary services is called reserve power. There are instants in the electricity market that selling the reserve power is more profitable than producing with the full capacity. Therefore wind turbines of a wind farm can be down regulated and the differential capacity can be traded as the reserve power. The total amount of energy that a wind farm can potentially generate is called possible power. It is very important for a wind farm owner to have a good estimate of the possible power of the wind farm in order to be able to trade the reserve power. The first two big offshore wind farms in Denmark, namely Nysted and Horns Rev 1, have already an extra signal in the SCADA data feed from the individual turbines called possible power. For calculating the possible power of the wind farm, the possible power of the individual wind turbines are added together. Traditionally the possible power of each wind turbine in a wind farm is calculated based on the filtered nacelle anemometer measurements. Then, the calculated values are added together to estimate the possible power of the whole wind farm. This approach normally results in a too optimistic possible power estimation. For example suppose the case when the possible power of the wind farm is calculated while the front row wind turbines are down-regulated and therefore their wake deficits are less on the down stream turbines. In this case the possible power of the front row gives a rather correct estimate, however since the downstream wind turbines see more wind in the down-regulated situation than the nominal situation, their possible power value is rather inaccurate, especially around the rated wind speed where as we will show in this work, this error is maximum. We show the difference between possible power of a wind farm calculated based on local wind speed measurements and the actual possible power. In this paper we use two methods of wind speed estimation to get a more accurate wind speed estimate

⋆ This work is supported by the Possible Power Project funded by the Danish Council for Strategic Research.

and compare our results. The outline of the paper is as follows: We will start by explaining the wind farm model in 2. This section contains the PI controller for down-regulation, the wake model and the wind farm layout. In section 3 we will explain the notion of possible power. For calculating possible power wind speed should either be measured or estimated. Therefore we will also discuss two methods of wind speed estimation in section 3.1. In section 4 simulations are given.

2. WIND FARM MODEL

In this section the wind farm model which is used for simulations will be presented. The wind farm consists of nonlinear model of a number of 5MW reference wind turbines (Jonkman et al., 2009). Details of modeling and the nonlinear model is given in (Mirzaei et al., 2012). Each of the turbines are augmented with a PI controller which is designed for controlling and de-rating the turbine. Each wind turbine model accepts time series of wind speeds (hub height wind speeds) and power set points and returns generated power, rotational speed, and C_p and C_t values of the operating point. The C_t values are used in the wake models to calculate wind speed on the down-stream wind turbines.

2.1 The PI controller for down-regulated turbines

The PI controller explained in (Jonkman et al., 2009) is modified to be suitable for down-regulating wind turbines. There are two ways of modifying the PI controller to follow the down regulation command. One method is to control the output power to follow the active power set point and keep the rotational speed constant at turbine's rated value. The other method is to modify the set points of both the output power and the rotational speed. For more details on the control strategies please see (Mirzaei et al., 2014). Both of these methods are implemented in the nonlinear model of the wind turbines.

2.2 Wake Modeling

The wake modelling is a sub-discipline of fluid dynamics that is focused on the aerodynamics of the flow behind the wind turbine(s). There are mainly two physical phenomena of interest in the wake: 1) the momentum (or velocity) deficit which causes a reduction in the power output of the downstream turbines 2) the increased level of turbulence which gives rise to unsteady loading on downstream turbines. These wake-induced power losses and blade loadings are studied in two regions within the wake namely near and far wake. The near wake starts right after the turbine and extends to 2-4 diameters downstream. In that region, the flow is highly characterized by the rotor geometry which leads to the formation of blade tip vortices. In addition to these tip vortices, because the turbine extracts momentum and energy from the flow, there exist steep gradients of pressure and axial velocity, and expansion of the wake. In the far wake on the other hand, the effects of the rotor geometry are limited to the reduced wind speeds and increased turbulence intensities. In fact, the turbulence is the dominating physical property in the far wake (Crespo and Hernandez, 1996). In addition to the rotor induced turbulence, the region further downstream is under the influence of the large scale (or atmospheric) turbulence. The turbulence mixing accelerates the wake recovery in terms of both the velocity deficit and the turbulence intensity. In far downstream, the velocity deficit approaches to a Gaussian profile which is axisymmetric and self-similar (Barthelmie et al., 2006), (Rados et al., 2001) . Moreover, the meandering of the wake might also contribute to the recovery of the velocity deficit whereas significantly increasing the unsteady loading on the downstream turbine(s). All these concepts and assumptions lead to different approaches used in the development of wake models and out of many, the N.O. Jensen Model has been used in this study.

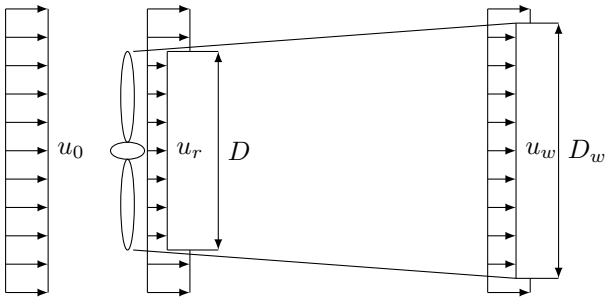

Fig. 1. The control volume considered in the N.O. Jensen model

N.O. Jensen Model: The N.O. Jensen model is one of the most popular wake models among engineering applications due to its simplicity, practicality and robustness. The information presented is based on the studies of N.O. Jensen (Jensen, 1983) and (Katic et al., 1987). Using the control volume presented in figure 1, and assuming a top-hat inflow profile (or rectangular profile as stated earlier) conservation of momentum is applied between the rotor plane and the downstream flow.

$$\left(\frac{D}{2}\right)^2 u_r^2 + \left[\left(\frac{D_w}{2}\right)^2 - \left(\frac{D}{2}\right)^2\right] u_0^2 = \left(\frac{D_w}{2}\right)^2 u_w^2 \quad (1)$$

Also, the wake is assumed to be expanded linearly as a function of the downstream distance x with a rate of 0.04 concluded in an expression of:

$$D_w = D + 2ax \quad (2)$$

By inserting equation 2 into 1, the normalized velocity can be found as:

$$\frac{u_w}{u_0} = 1 - \frac{2a}{(1 + 2ax/D)^2} \quad (3)$$

where a is the axial induction factor which can be expressed for that control volume as; $a = 1 - u_r/u_0$ which is also related with the thrust coefficient (Hansen, 2008), c_T, as $c_T = 4a(1-a)$. Solving for:

$$a = \frac{1 - \sqrt{1 - c_T}}{2} \quad (4)$$

Substituting equation 4 into 3, the velocity deficit can be described as;

$$\Delta u = 1 - \frac{u_w}{u_0} = \frac{1 - \sqrt{1 - c_T}}{(1 + 2ax/D)^2} \quad (5)$$

As mentioned earlier, each wind turbine gets time series of wind speeds and demanded power as inputs and returns several times series as outputs. c_T is one of the output

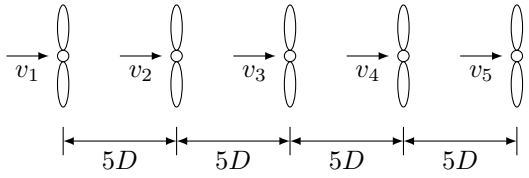

Fig. 2. Wind farm layout

values which is used in the wake models. Therefore for a wind farm simulation we start by simulating the first wind turbine, and by calculating the outputs, having the distance to the second wind turbine in the row and using the wake model explained above, the time series of the wind speed on the second wind turbine can be calculated. This approach is repeated on each individual machine to the last wind turbine in the row. A window of specific size is chosen and its mean wind speed is used to calculate the transition delay of the wake from the upstream wind turbine the the downstream one.

2.3 The wind farm layout

This is a simple simulation case, therefore a simple wind farm with 5 wind turbines in a row is considered. The wind direction is such that the wind turbines are in the full wake of the front row turbines. The distance between the turbines are considered to be $5D$ as shown in figure 2.

3. POSSIBLE POWER

As mentioned earlier, currently the possible power of a wind farm is calculated as a sum over the possible power of the individual turbines in the farm:

$$\mathcal{P}_{poss} = \sum_{i=1}^{N} \mathcal{P}_i \tag{6}$$

in which N is the number of the turbines in the wind farm, $\mathcal{P}_{poss}$ is the possible power of the wind farm, and $\mathcal{P}_i$ is the possible power of an individual wind turbine. In order to have a measure of the possible power of the individual wind turbines, the effective wind speed (v_e) on the turbine should be measured or estimated. In section 3.1 two wind speed estimation approaches are given. Thereafter the estimated or measured wind speed is used to calculated the possible power ($\mathcal{P}_i$) using the power curve of the turbine. The power curve of the $5MW$ reference wind turbine (Jonkman et al., 2009) is given in figure 3.

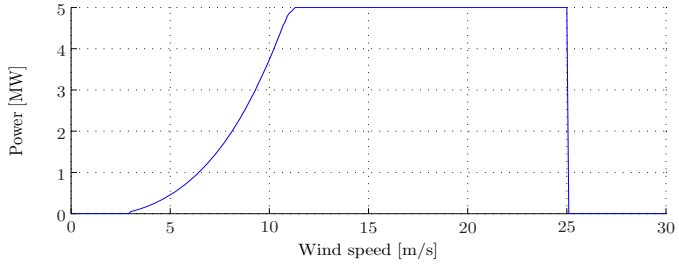

Fig. 3. Power curve for the 5MW reference wind turbine

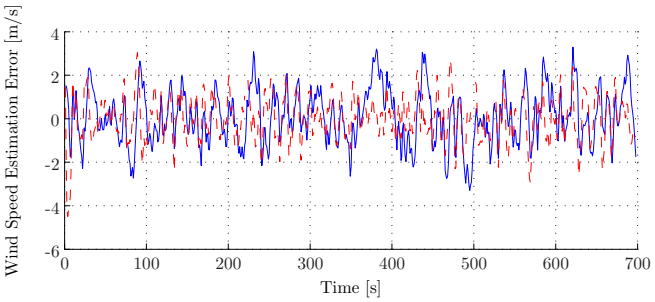

Fig. 4. Error in the estimation of the wind speed (solid-blue EKF method and red-dashed power balance method)

3.1 Wind speed estimation

One way for calculating the possible power, is to measure the wind speed by nacelle based anemometers. However it is known that the anemometer measurements are not reliable enough as there are many sources of error in their measurements (Diznabi, 2009). The anemometers are placed on the nacelle and therefore their measurements are heavily influenced by the induction of the rotor. The induction itself depends on many factors such the rotational speed of the rotor, the wind speed and the pitch of the blades. A better way for measuring the effective wind speed is to use the whole rotor as a measurement device. A method based on Extended Kalman filter is presented in (Mirzaei et al., 2012). In this section another method for estimating the effective wind speed for large wind turbines is presented. In this approach, a secant root finding algorithm is used to solve the power equation of the turbine and therefore the effective wind speed is calculated. The method is called *the power balance approach*. In this approach the wind speed is estimated by solving the following equation:

$$\frac{1}{2}\rho\pi R^2 \mathcal{V}_e^3 C_p(\Theta, \Omega_r, \mathcal{V}_e) = \mathcal{P}_e \tag{7}$$

In this equation C_p curve is given and Θ, Ω_r and $\mathcal{P}_e$ are measured. We have used a secant root finding algorithm to solve the equation and find $\mathcal{V}_e$. Figure 4 shows a comparison of the estimation error of the Extended Kalman filter and the power balance methods. As it could be seen, the power balance method gives an estimation with lower variance, but higher oscillations in the error and the EKF method gives an estimation with bigger excursion in the error and less oscillations. The performance of the EKF depends on its tuning and actually that is one of the pitfalls of using the EKF method while the power balance method does not need tuning. Besides, the EKF method might run into instability and it is computationally too expensive, while the power balance method does not have these shortcomings. A presentation of different wind speed estimation methods and a comparison among them is also given by Soltani et al. (2013).

3.2 Possible power estimation (algorithm)

We defined the possible power $\mathcal{P}_{poss}$ in the beginning of this section, here we define a new parameter $\mathcal{P}^*_{poss}$ which is the possible power calculated by taking the effect of the reduced wake deficit of the down-regulated wind turbines into account. When the wind turbines are down-regulated, their wake deficit is smaller and therefore on

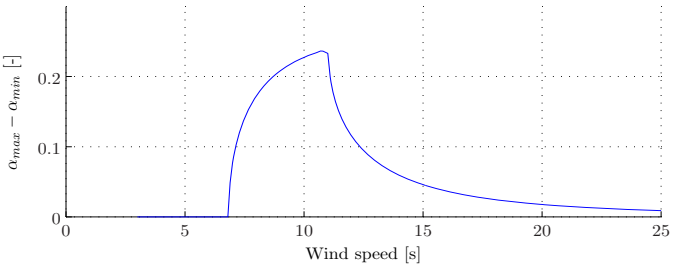

Fig. 5. Difference between the maximum and the minimum induction factor

the downstream wind turbines a higher wind speed is seen. $\mathcal{P}^*_{poss}$ is more realistic and in different simulation scenarios we will show that it gives a better measure of the possible power and that the possible power calculated as in equation (6) is in the case of down-regulation too optimistic. For calculating $\mathcal{P}^*_{poss}$, we employ an iterative method in which we start with the front row wind turbine and calculate its operating point based on the available wind speed v_1 and its nominal power. Therefore we can find the generated power for the turbine $\mathcal{P}^*_1$ and its thrust coefficient c_{T1}. Having c_{T1}, we calculate the wake deficit on the wind turbine of the second row (v_2) and repeat the same procedure for the rest of the turbines. Using this algorithm for calculating the possible power of the individual wind turbines $\mathcal{P}^*_i$, we can calculate the possible power ($\mathcal{P}^*_{poss}$) of the whole wind farm:

$$\mathcal{P}^*_{poss} = \sum_{i=1}^{N} \mathcal{P}^*_i \tag{8}$$

4. WIND FARM SIMULATIONS

In this section different simulation scenarios are presented to show the effect of wake on the measured possible power of a down-regulated wind farm $\mathcal{P}_{poss}$ and the estimated possible power $\mathcal{P}^*_{poss}$ explained in section 3.2. As it is seen in section 2.2.1, the wind deficit in the wake of a turbine depends directly on the induction factor of the rotor given in equation 4. The difference between $\mathcal{P}_{poss}$ and $\mathcal{P}^*_{poss}$ depends on the difference between the induction factor of the down-regulated wind turbine and the nominal operation. Figure 5 shows the difference between the maximum induction factor of the reference wind turbine at the nominal operating point and the minimum induction factor at down-regulated to 20% of the nominal capacity. As it can be seen in the figure, the difference has its peak around the rated wind speed, and it becomes small for both low and high wind speeds. It is small for the low wind speed because the operating points of the turbine is basically the same as long is it has not reached the down-regulated power set point and therefore the induction factors are equal. For the higher wind speed the operating points of the down-regulated case and the nominal case are close and therefore the difference between the induction factors becomes small. Three simulation scenarios are given to show the difference between $\mathcal{P}_{poss}$ and $\mathcal{P}^*_{poss}$ for different operating regimes.

4.1 Constant wind speed, steps in the power set point

In this simulation scenario wind speed is kept constant at $13m/s$, just above the rated wind speed (see figure 6). The power set point of the wind farm is increased stepwise (see figure 8). In this simulation scenario the demanded power is spread between the turbines equally. As it is seen in figure 8, when the wind farm is producing with 20% of its capacity, the possible power in the wind farm appears to be $\mathcal{P}_{poss} = 25MW$. This is because the possible power of the individual wind turbines are measured to be $5MW$ (see figure 7). As the wind turbines are operating only at 20% of their capacity, the wake deficit is not big enough to reduce the wind speed on the down-stream wind turbines below their rated values. However when the power set point is increased stepwise, at time 550 we start to see that the possible power $\mathcal{P}_{poss}$ starts to decrease. At time 1200 the wind farm is producing its maximum power which is the possible power $\mathcal{P}^*_{poss}$ and it is no longer able to follow the power set point. Algorithm given in section 3.2 is used to calculate $\mathcal{P}^*_{poss}$ and it gives a value of $17.2MW$ which we see at time 1000 is the correct value. Figure 9 shows the generated power of the individual wind turbines and as it is seen when the generated power of the front row wind turbines are increased, the downstream wind turbines are no longer able to follow the power set point.

4.2 Constant nominal power set point, steps in the wind speed

In this simulation scenario the power set point is kept constant at its nominal value (see figure 12) and the wind speed is increased stepwise from $13m/s$ to $20m/s$ (see figure 10). The generated power for the individual wind turbines are given in figure 13. In this simulation scenario, as the wind turbines are operating with their nominal capacity and the wake deficit is the maximum, the two possible power measures ($\mathcal{P}^*_{poss}$ and $\mathcal{P}_{poss}$) and the

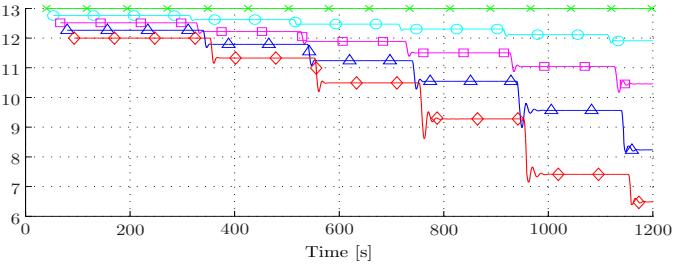

Fig. 6. Wind speed on the individual wind turbines (green-cross curve shows the wind speed of the first turbine in the row and red-diamond curve shows the wind speed of the last turbine)

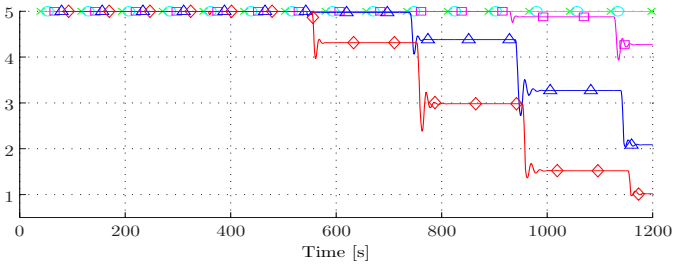

Fig. 7. Possible power of the individual wind turbines, $\mathcal{P}_i$ (green-cross curve shows the possible power of the first turbine in the row and red-diamond curve shows the possible power of the last turbine)

generated power are the same, see figure 12. An interesting fact which was explained before in the difference between the maximum and the minimum induction factor can be seen in the wind speed measured on each wind turbine in figure 10. This figure shows as the wind speed increases, the wake deficit decreases and therefore the difference between the wind speed on the front row turbine with the last row turbine decreases. Figure 13 shows the generated power of the individual wind turbines and as it is seen until time 350 when the wind speed reaches $15m/s$ last row wind turbines are not able to produce the nominal value.

4.3 Constant down-regulated power set point, steps in the wind speed

In this simulation scenario the power set point is kept constant at 20% of its nominal value (see figure 16) and the wind speed is increased stepwise from $13m/s$ to $20m/s$ (see figure 14). The generated power for the individual wind turbines are given in figure 17. In this simulation scenario, as the wind turbines are operating with 20% of their nominal capacity and the wake deficit is the minimum, the possible power $\mathcal{P}_{poss}$ is incorrectly measured to be $25MW$. However $\mathcal{P}^*_{poss}$ correctly shows that maximum wind farm capacity of $25MW$ is not achieved until time 400 when wind speed reaches $15m/s$, see figure 16.

5. CONCLUSION

We explained that a correct measurement of the possible power of a wind farm is beneficial for providing reserve service for the grid. And also we demonstrated that calculating possible power of a wind farm by aggregating possible power of individual wind turbines lead to an error. This error can increase the uncertainty in the

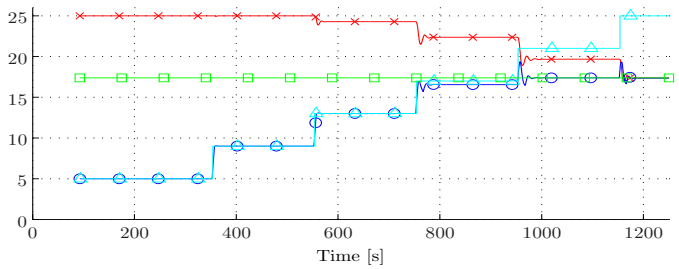

Fig. 8. Blue-circles curve is wind farm power, red-cross curve is possible power ($\mathcal{P}_{poss}$), cyan-triangles curve is the power set point for the wind farm and green-square curve shows the possible power of the wind farm ($\mathcal{P}^*_{poss}$) calculated by the presented algorithm, all in MW

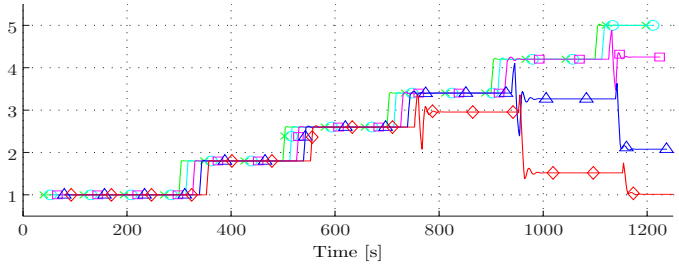

Fig. 9. Generated power of the individual wind turbines (green-cross curve shows the generated power of the first turbine in the row and red-diamond curve shows the generated power of the last turbine)

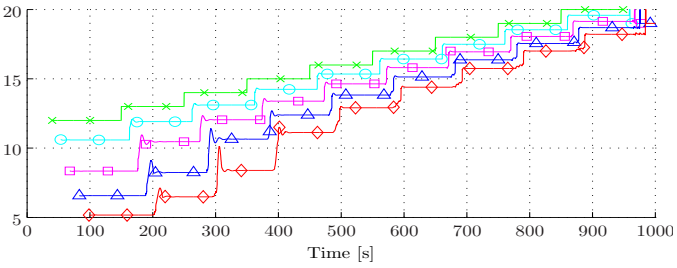

Fig. 10. Wind speed on the individual wind turbines (green-cross curve shows the wind speed of the first turbine in the row and red-diamond curve shows the wind speed of the last turbine)

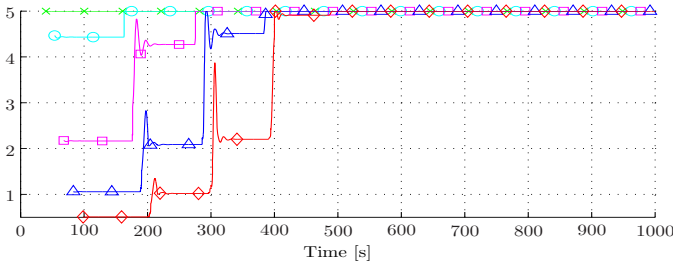

Fig. 11. Possible power of the individual wind turbines, $\mathcal{P}_i$ (green-cross curve shows the possible power of the first turbine in the row and red-diamond curve shows the possible power of the last turbine)

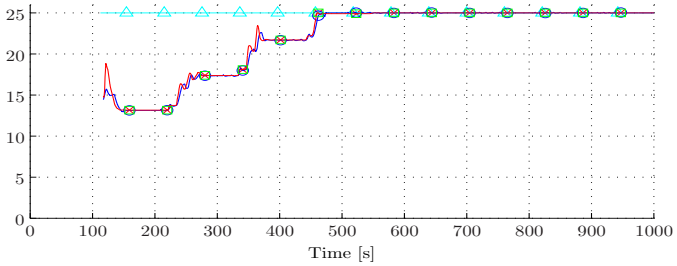

Fig. 12. Blue-circles curve is wind farm power, red-cross curve is possible power ($\mathcal{P}_{poss}$), cyan-triangles curve is the power set point for the wind farm and green-square curve shows the possible power of the wind farm ($\mathcal{P}^*_{poss}$) calculated by the presented algorithm, all in MW

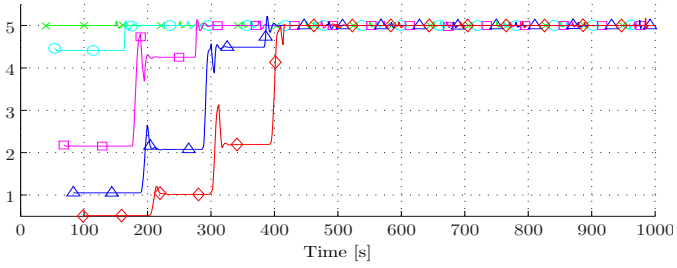

Fig. 13. Generated power of the individual wind turbines (green-cross curve shows the generated power of the first turbine in the row and red-diamond curve shows the generated power of the last turbine)

possible power estimation of the wind farm. We have also shown that this error is specially significant around the rated wind speed of the turbine where the induction

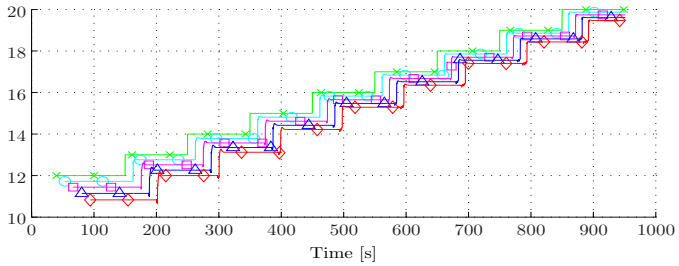

Fig. 14. Wind speed on the individual wind turbines (green-cross curve shows the wind speed of the first turbine in the row and red-diamond curve shows the wind speed of the last turbine), all in m/s

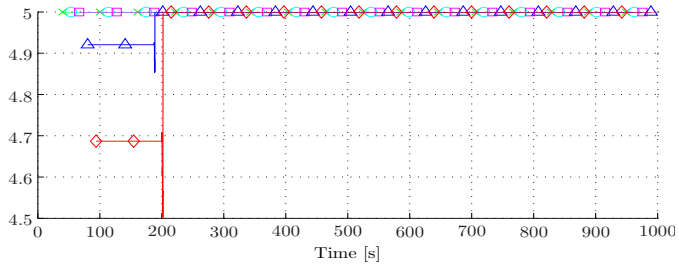

Fig. 15. Possible power of the individual wind turbines ,P_i (green-cross curve shows the possible power of the first turbine in the row and red-diamond curve shows the possible power of the last turbine), all in MW

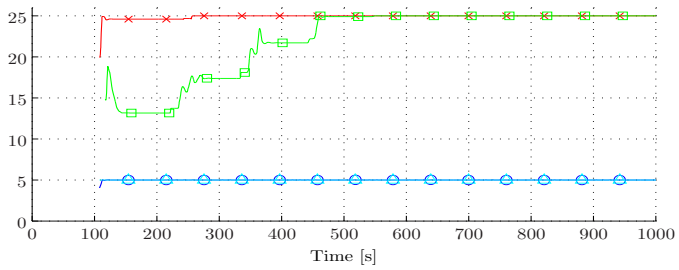

Fig. 16. Blue-circles curve is wind farm power, red-cross curve is possible power ($\mathcal{P}_{poss}$), cyan-triangles curve is the power set point for the wind farm and green-square curve shows the possible power of the wind farm ($\mathcal{P}^*_{poss}$) calculated by the presented algorithm, all in MW

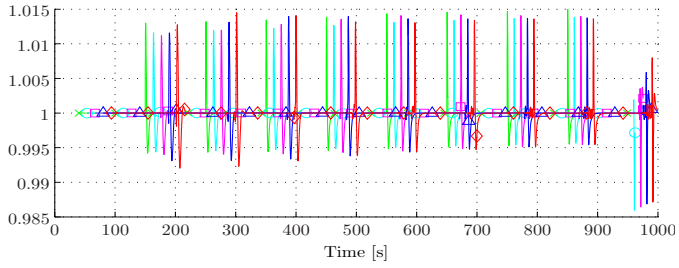

Fig. 17. Generated power of the individual wind turbines (green-cross curve shows the generated power of the first turbine in the row and red-diamond curve shows the generated power of the last turbine), all in MW

factor has its highest values. We also presented a simple algorithm for calculating the possible power of a row of wind turbines and showed by simulations that for different wind speeds and power set points the algorithm gives a better estimation of the possible power.

REFERENCES

Aho, J., Buckspan, A., Laks, J., Dunne, F., Pao, L., Fleming, P., Churchfield, M., Jeong, Y., and Johnson, K. (2012). A tutorial of wind turbine control for supporting grid frequency through active power control. *Proc Am Control Conf*, 3120–3131.

Barthelmie, Folkerts, Larsen, Rados, Pryor, Frandsen, Lange, and Schepers (2006). Comparison of wake model simulations with offshore wind turbine wake profiles measured by sodar. *J. Atmos. Ocean. Technol. (USA)*, 23(7), 888–901.

Crespo, A. and Hernandez, J. (1996). Turbulence characteristics in wind-turbine wakes. *Journal of wind engineering and industrial aerodynamics*, 61(1), 71–85.

Diznabi, B. (2009). *Investigation of the flow relation to nacelle anemometry*. Master's thesis, Technical University of Denmark, DTU, DK-2800 Kgs. Lyngby, Denmark.

Hansen, A.D. (2010). Evaluation of power control with different electrical and control concept of wind farm. Technical report, Technical University of Denmark.

Hansen, M.O.L. (2008). *Aerodynamics of Wind Turbines*. Earthscan.

Jensen, N. (1983). A note on wind generator interaction. Technical report, Risø.

Jonkman, J., Butterfield, S., Musial, W., and Scott, G. (2009). Definition of a 5MW reference wind turbine for offshore system development. Technical report, National Renewable Energy Laboratory,, 1617 Cole Boulevard, Golden, Colorado 80401-3393 303-275-3000.

Katic, I., Højstrup, J., and Jensen, N. (1987). A simple model for cluster efficiency. *EWEC'86. Proceedings. Vol. 1*, 407–410.

Miller, N.W. and Clark, K. (2010). Advanced controls enable wind plants to provide ancillary services. *IEEE Power & Energy Society General Meeting*, 1–6.

Mirzaei, M., Poulsen, N.K., and Niemann, H.H. (2012). Robust model predictive control of a wind turbine. In *American Control Conference*. Montral, Canada.

Mirzaei, M., Soltani, M., Poulsen, N.K., and Niemann, H.H. (2014). Model based active power control of a wind turbine. In *American Control Conference*. Portland, OR, the United States.

Rados, Larsen, Barthelmie, Schlez, Lange, Schepers, Hegberg, and Magnisson (2001). Comparison of wake models with data for offshore windfarms. *Wind Eng. (UK)*, 25(5), 271–280.

Rebours, Y.G., Kirschen, D.S., Trotignon, M., and Rossignol, S. (2007). A survey of frequency and voltage control ancillary servicespart i: Technical features. *IEEE Trans. Power Syst.*, 22(1), 350–357.

Soltani, M.N., Knudsen, T., Svenstrup, M., Wisniewski, R., Brath, P., Ortega, R., and Johnson, K. (2013). Estimation of rotor effective wind speed: A comparison. *IEEE Trans. Contr. Syst. Technol.*, 21(4), 1155–1167.